Microstructural control on the P-T path construction in metapelites from the Austroalpine crust (Texel Gruppe, Eastern Alps)

Dedicated to the memory of Ugo Pognante, Torino 1954 – Mont Blanc du Tacul 1992

by *Maria Iole Spalla*[1]

Abstract

In the metapelites of the Austroalpine Texel Gruppe a sequence of metamorphic reactions synkinematic with successive regional deformation phases (D1, D2 and D3) can be identified by microstructural analysis and by mapping of structures. The thermobarometric estimates obtained by this method are used to derive a retrograde P-T-*relative time of deformation* path. The resulting P-T boxes are relatively small, i.e. 0.9–1.0 GPa / 640–680 °C for stage D1, and 0.6–0.75 GPa / 550–580 °C for stage D2. During D3 a greenschist retrogradation took place with P < 0.4 GPa and T < 500 °C. When microstructural controls are not considered larger P-T intervals are obtained (e.g. 550 < T < 680 °C or more for garnet-biotite pairs). Utilizing available radiometric data allows to assign an Alpine age at least to the D2 and D3 tectonometamorphic stages which represent the uplift of this part of the Austroalpine crust from a depth ≥ 30 km.

Keywords: metapelite, thermobarometry, microstructure, P-T-t path, metamorphic evolution, Texel Gruppe, Eastern Alps.

Introduction

The recognition of several stages of the structural and metamorphic evolution of basement units has been fruitfully applied for tracing the tectonic history of the Alpine chain (e.g. HIGGINS, 1964; HALL, 1972). When this approach to trace the timing of mineral growth in relation to the deformation history is used, metamorphic investigations must be supported by careful structural analysis in the field and by detailed microstructural work. For this purpose it is important to distinguish groups of geometries which are regionally significant in the field and which define the chronology among the superposed structures (e.g. GOSSO, 1977; HUBER et al., 1980). In addition, finite strain is generally heterogeneous in deformed rocks (RAMSAY and GRAHAM, 1970). Within an orogenic tectonite partitioning of strain generates domains of extremely limited deformation at the scale of grain size (where *coronitic textures* form during metamorphism), as well as domains where growth of new minerals is accompanied by pervasive foliation development *(tectonitic textures)* and domains of localized high strain where syn-metamorphic *mylonitic textures* develop (e.g. HOBBS et al., 1976; LARDEAUX and SPALLA, 1990).

Actually the most recurrent structural association in metamorphic terrains displays the coexistence of coronites, tectonites and mylonites, generated in time during the same phase of deformation and related in space by strain gradients. For this reason the individual definition of zones where different deformation mechanisms are contemporaneously active is fundamental in selecting samples since the microstructural location of individual mineral grains influences the evolution of their chemical composition (CIMMINO and MESSIGA, 1979; LARDEAUX et al., 1983; MØRK, 1985).

In addition BELL and co-workers (1986) proposed a general model of deformation partitioning at the scale of grain size. The model distinguishes sites where nucleation and growth of new

[1] Dipartimento di Scienze della Terra, Università degli Studi, Via Mangiagalli 34, I-20133 Milano, Italy.

Legend:

- **Northern Calcareous Alps**
- **Paleozoic and Quartz-phyllites of the Steinach Nappe**
- **Massif of the Brixen Granite**
- **Crystalline Basement of the Southern Alps**
- **Innsbruck Quartzphyllites**
- **Penninic Zone undetailed including Matrei Zone**
- **Micaschists and Paragneisses**
- **Orthogneisses**
- **Amphibolites**
- **AMA** Alpine mica ages
- **Ö** Ötztal
- **C** Campo
- **Schneeberg Complex (micaschists, marbles, etc.)**
- **Low grade retrogressed basement**
- **Central-alpine Mesozoic**
- **✳** Alpine eclogites of Saltaus
- **PA** Periadriatic Lineament
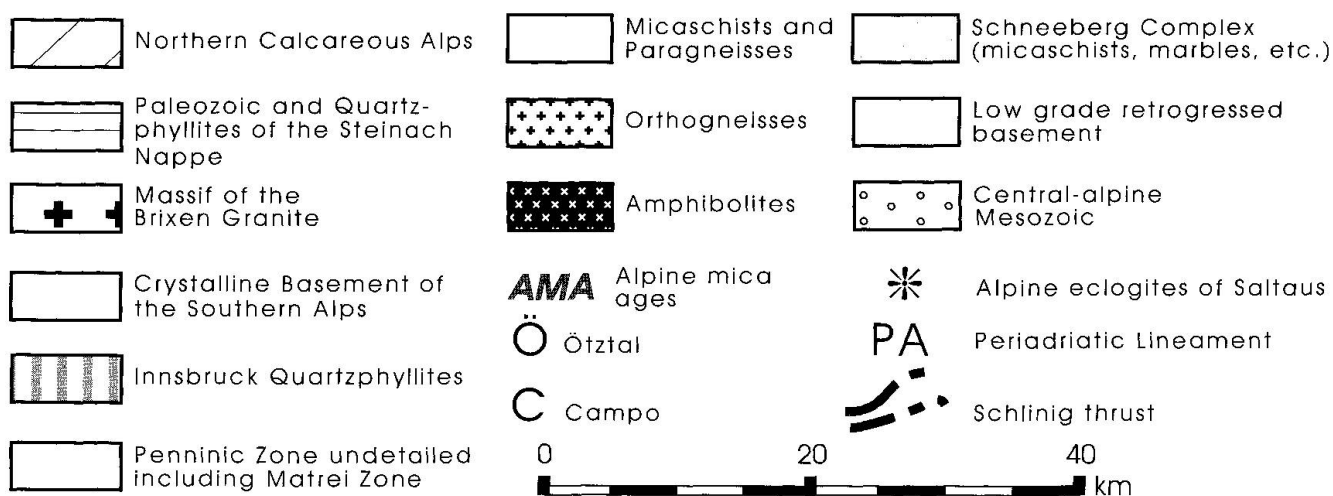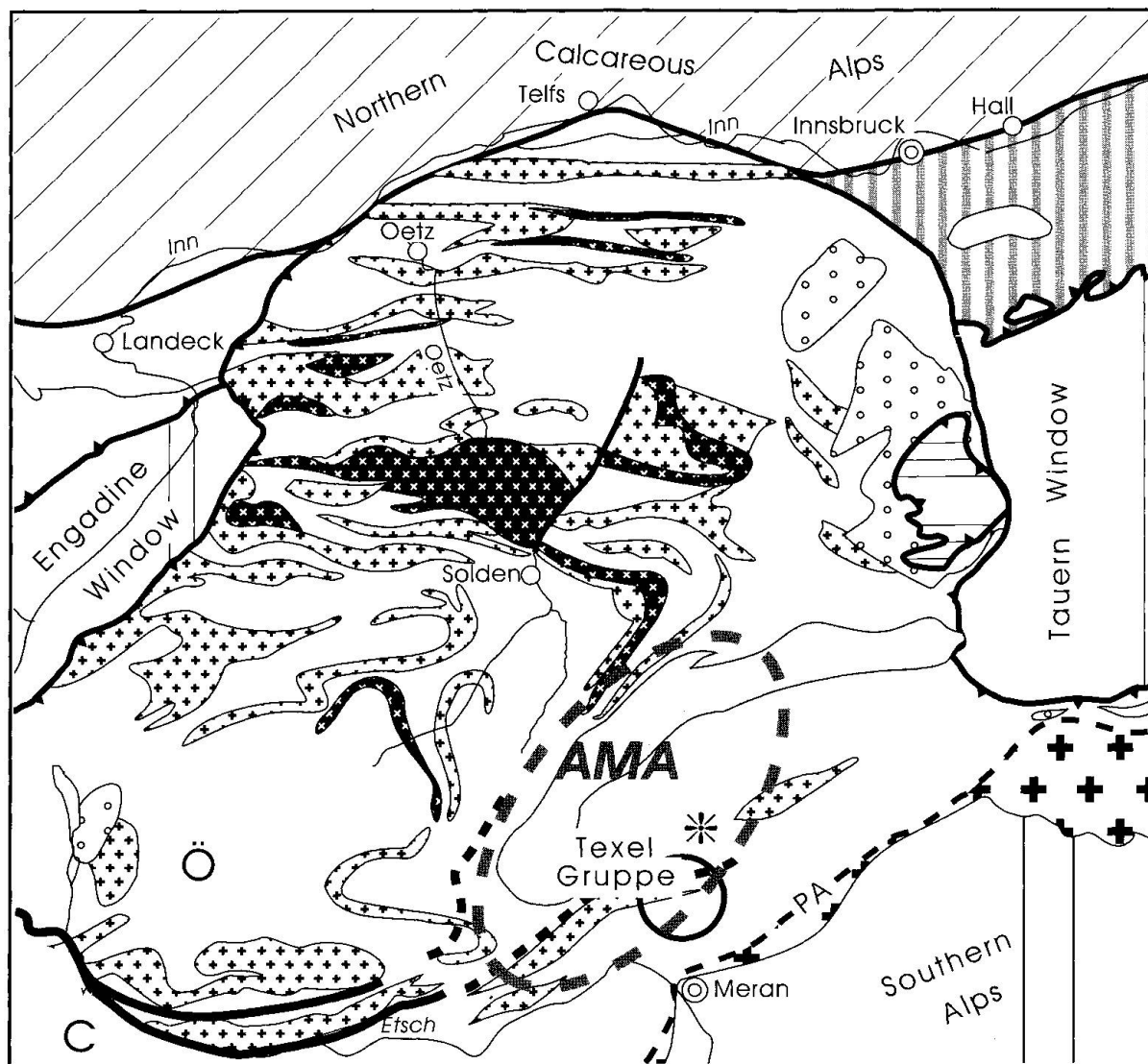- Schlinig thrust

0   20   40 km

Fig. 1   Tectonic sketch map of the Austroalpine domain in the Central-Eastern Alps redrawn after ANGENHEISTER et al. (1972). The Schlinig Thrust is located on the map according to SCHMID and HAAS (1989); the open circle locates the area. Saltaus eclogites after HOINKES et al. (1991) and AMA after THOENI and HOINKES (1987).

mineral phases are favoured from sites showing preserved relics or dominating dissolution and intracrystalline plasticity. They subdivide the development of a new foliation into successive stages (BELL and RUBENACH, 1983; BELL and HAYWARD, 1991) from crenulation to complete obliteration of the original fabric (decrenulation; BELL, 1986).

In this study the polydeformed metapelites of the Texel Gruppe are regarded as most favorable rocks for utilizing porphyroblast-matrix relationships to derive the timing of mineral growth with respect to foliation development and to define microdomains in which specific deformation mechanisms dominate. A sequence of metamorphic reactions is deduced and thermobarometric estimates are obtained in carefully selected microdomains.

Fig. 2 Interference pattern of D2 overprinting D1 folds in a metagranitoid dyke. The S2 foliation is the prevailing element within this composite fabric. Laghi del Latte, Spronsertal.

Geological Setting

The Texel Gruppe belongs to the Upper Austroalpine continental crust (FRANK, 1987) and is comprised between the Tauern window and the Schneeberg-Laas Complex. It has been considered either as a part of the Ötztal nappe (ANGENHEISTER et al., 1972; FRANK et al., 1987) or as a portion of the Campo unit (SCHMID and HAAS, 1989) near the boundary between the Ötztal and Campo units, and more precisely within the intrabasement shear zone considered as the deep prolongation of the Schlinig thrust (Fig. 1). Although high pressure–high temperature assemblage in metapelites (SPALLA, 1989b) and eclogitic relics in amphibolites have been recently discovered (HOINKES et al., 1991; POLI, 1989), the debate Alpine versus pre-Alpine age of the main metamorphic imprint in this portion of the Austroalpine crust is still open. In the past the metamorphism affecting the Upper Austroalpine crust was interpreted essentially as a thermal event (e.g. FRANK, 1987; FRISCH, 1979), both during Alpine and pre-Alpine time, and nobody has yet tried to propose an orogenically coherent geodynamic model to explain the high pressure metamorphism.

Intimate intercalations of metasedimentary rocks (paragneisses, micaschists, quartzites and marbles) with amphibolites and metagranitoids represent good structural markers at the meso and mega scale (Fig. 2). Numerous field investigations were performed in this part of the Alpine chain and different polyphased structural evolutions with various interpretations of deformation-metamorphism relationships were deduced. For a critical review of the debated interpretations the reader is referred to the paper of VAN GOOL et al. (1987). Particularly for the Texel Gruppe region

SPALLA (1990a) gives a detailed description of the complex structural evolution, that will be briefly summarized below.

The D1 structures are represented by a relic foliation or by rootless metric folds. D2 corresponds to isoclinal folding, associated with a pervasive axial plane foliation (Fig. 2); in the metapelitic rocks sheath-like folds and mylonitic bands develop and a stretching lineation is underlined by biotite, feldspar, quartz and minor white mica. In the orthogneiss D2 is characterized by conjugate shear bands, mainly defined by biotite and white mica. D3 is associated with a regional recumbent fold system and during this phase a reactivation of the pre-existing fabric elements took place. The dominant sense of asymmetry is coherent with the sense of shear in the ductile shear zones and it gives a top to the South-East direction of movement. The stretching lineation is constituted by chlorite, white mica and quartz.

Conjugate kink-bands and chevron folds sporadically occur and overprint D3 structures that are crosscut by a grid of extensional cataclastic bands. They are distinguished by the concentration of calcite, chlorite and sometimes graphite. Small scale widespread joints are related to these latter structures, showing the same orientation and mineralogical association.

Microstructural analysis

The microstructural analysis of the Texel metapelites (micaschists and paragneisses) is based on the dynamic method to distinguish mineral growth with respect to relative time of deformation as proposed by BELL et al. (1986). It is also
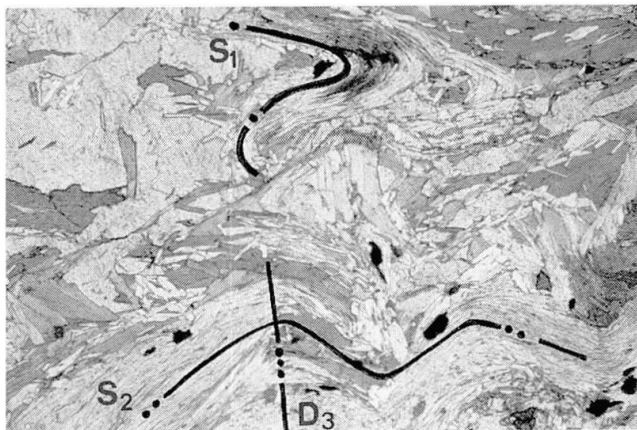
Fig. 3 Progressive decrenulation during D2 by elimination of S1 relic micas (vertical individuals at center of the image). S2 has a horizontal envelope, being crenulated by D3, with vertical axial plane. Paragneiss, Lago Catino, Spronsertal. Horizontal edge = 3,5 mm.

important to refer to the classical methods largely utilized in the microstructural analysis of metamorphic tectonites (FERGUSON and HARTE, 1975; POWELL and VERNON, 1979; VERNON, 1976).

The structural pattern well recognizable at the meso and megascale (Fig. 2) is well represented

also at the microscale, where the earliest foliation (S1) is marked by the alignment of biotite and white mica which are stable also during the second phase of folding, as evidenced by biotite and white mica which are always aligned along S2. Both these foliations are affected by F3 crenulation (Fig. 3).

Where the S2 foliation is more evolved and the S1 micaceous relics in microlithons are nearly completely obliterated, biotite porphyroclasts occur with dimensional orientation parallel to S2 foliation, but the (001) cleavage forms a high angle with S2. Here subgrains (low misfit subgranular cells) and new grains form and their margins are overgrown by newly oriented biotite (Fig. 4a). The same process occurs in white mica porphyroclasts (Fig. 4b).

Garnet porphyroblasts preserve relics of the earlier foliation marked by quartz, plagioclase, micas and rutile, that form a high angle with the S2 foliation. Relics of K-feldspar are still preserved as inclusions within garnet. Biotite and white mica often occur in the pressure shadows of garnet. Rutile is often rimmed by ilmenite when it is enclosed in garnet or moulded in kyanite. Garnet is rimmed by kyanite and quartz. Ilmenite and
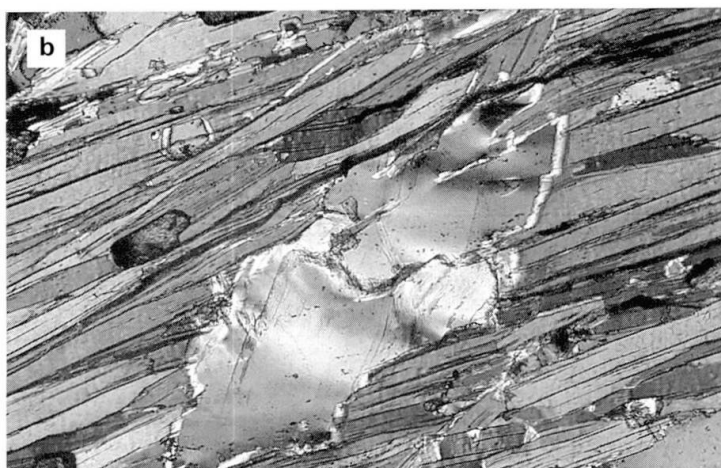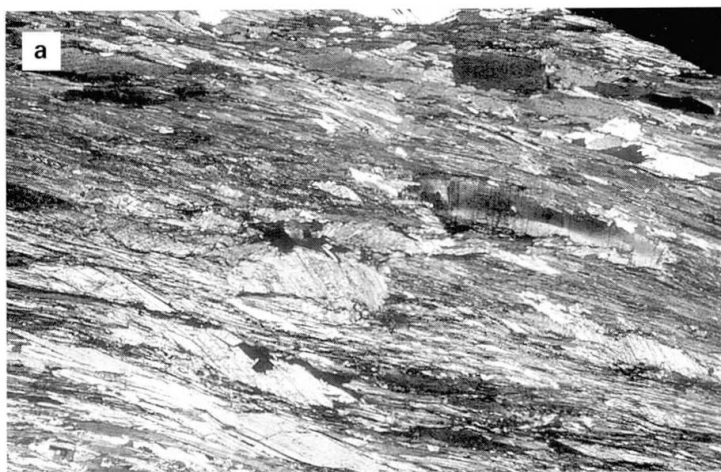
Fig. 4 (a) Intense grain size reduction in biotites by recrystallization, and reorientation along the S2 foliation of the new individuals, at the expense of larger biotite porphyroclasts. Paragneiss, Lago Catino, Spronsertal. (b) The same reorientation process as in figure 4a taking place in white micas. Note consumption of the porphyroclast by the newly growing, optically strain free grains. Paragneisses of Lago Catino, Spronsertal. (c) Growth of staurolite at microdomains of prevailing shear strain corresponding to white mica films. Kyanite-staurolite paragneiss; Spronserscharte, Spronsertal.
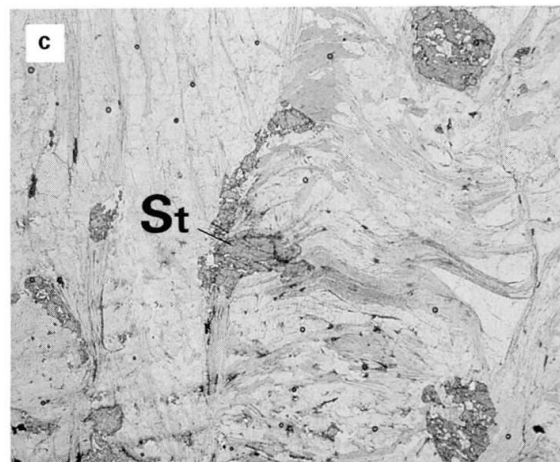
kyanite grow at the expense of garnet and rutile as explained by the reaction

$$Alm + Rt = Ilm + Ky + Qtz \qquad (a)$$
(BOHLEN et al., 1983).
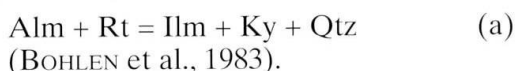
Kyanite is oriented parallel to the S1 pervasive foliation; its growth occurs at a late stage with respect to the S1 development, but it remains stable almost until the growth of staurolite during the final stages of S2 development. This is shown in figures 4c and 5a, where staurolite growth appears to be guided by intense localized shear strain (= phyllosilicate-rich films) during advanced decrenulation. Often staurolite develops at the rims of garnet and kyanite, sometimes giving rise to moulded structures. Plagioclase porphyroblasts, rarely twinned and with high relief, are elongated parallel to the S2 foliation and show undulose extinction. In D2 microlithons plagioclase grows at the rims and in the pressure shadows of garnet, and often develops along kyanite cleavage. These textural relations suggest that staurolite and plagioclase development may be associated to the reactions

$$Grs + Ky + Qtz = An \qquad (b)$$
(GHENT, 1976; HAYS, 1967)

$$Ky + Bt + Grt + V = St + Ms + Qtz \quad (c)$$
(CARMICHAEL, 1978)

or

$$Alm + Ms = St + Bt + Qtz \qquad (c')$$
(RAO and JOHANNES, 1979).
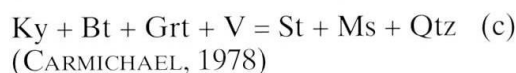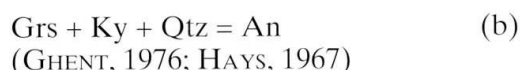
During the third phase of deformation a greenschist retrogradation took place with the development of chlorite in the openings along (001) of white mica a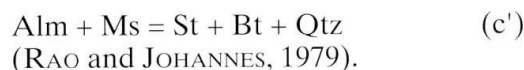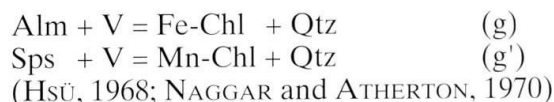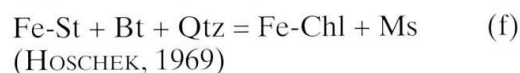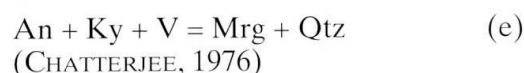nd biotite (Fig. 5a). Green biotite with chlorite, sericite and quartz develops in microfractured garnet, margarite develops at the expenses of kyanite (Fig. 5b). Reactivation of S2 planes takes place, accompanied by the growth of sericite and chlorite at the expenses of the amphibolite facies minerals (Fig. 5c). Plagioclase porphyroblasts develop syn-kinematically to D3 and overgrowing syn-D3 crenulated white micas. The development of chlorite, sericite and margarite at the expenses of garnet, biotite, staurolite, white mica, kyanite and plagioclase, during D3 deformation, suggest that reactions as

$$Bt + Grt + Ky = Chl + Ms + Qtz \qquad (d)$$
(HIRSCHBERG and WINKLER, 1968)

$$An + Ky + V = Mrg + Qtz \qquad (e)$$
(CHATTERJEE, 1976)

$$Fe\text{-}St + Bt + Qtz = Fe\text{-}Chl + Ms \qquad (f)$$
(HOSCHEK, 1969)
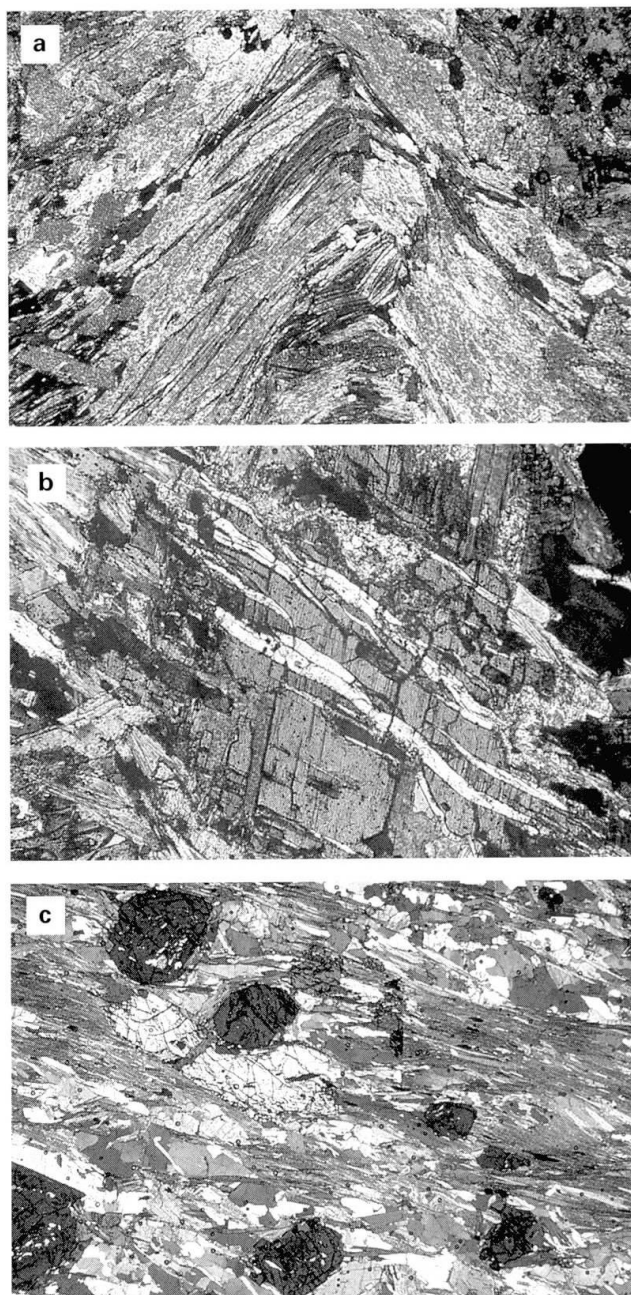
Fig 5 (a) Chlorite growth within (001) openings of phyllosilicates during D3. Micaschists of Lago Catino, Spronsertal. (b) Margarite growth through destabilization of kyanite porphyroblasts during D3 reactivation of S2 foliation. (c) Microboudinage of staurolite oriented along S2. Slightly rotated S2 trails are included as an Si (internal foliation) at staurolite margin (center of photo) and indicate a growth during late-D2 for staurolite. Chlorite grows during D3 reactivation of the S2 planes and in the necks of the microboudins of staurolite, in the S2 foliation and in the garnet pressure shadows. Staurolite micaschists, Lago Catino, Spronsertal.

$$Alm + V = Fe\text{-}Chl + Qtz \qquad (g)$$
$$Sps + V = Mn\text{-}Chl + Qtz \qquad (g')$$
(HSÜ, 1968; NAGGAR and ATHERTON, 1970)

occur.

Tab. 1 Deformation vs mineral growth in paragneisses and micaschists. Vertical stripes localize (a) to (h) reactions listed in the text.

MINERALS	D1	D2	D3
Quartz			
Plagioclase		olig/and	
K-feldspar ?	?		ab/olig
Garnet		Alm, Grs decrease	
Biotite		Pyr increase	green bt
White mica			
Rutile			
Ilmenite			
Kyanite			
Staurolite			
Chlorite			
Margarite			
Sericite			
Epidote			
Goethite			
Tourmaline			

h   a   b,c   d,e, f, g

In addition, the coexistence of garnet and K-feldspar, as relics of the early stage of the metamorphic evolution, and the occurrence of biotite and white mica in the S1 micaceous films may suggest the reaction

Grt + Kfs = Ms + Bt + Qtz   (h)
(VIELZEUF, 1984)
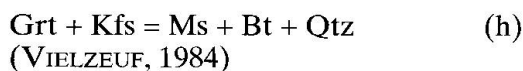
testifying a higher P-T stage during pre- or early-D1 deformation.

The stable assemblages during the successive phases of deformation are summarized in table 1, where appearance and duration of mineral phases are related to the deformation stages. The older minerals, as K-feldspar, plagioclase, quartz, biotite, white mica and rutile occur mainly as inclusions in garnet, and their growth partly predates D1. Rutile is replaced by ilmenite during D1, to which kyanite growth is also associated (reaction a). At the end of D1 the new assemblage is quartz, garnet, biotite, white mica, ilmenite and kyanite. During D2 new plagioclase and staurolite grow (reactions b and c) together with tourmaline giv-

ing rise to the association quartz, garnet, biotite, white mica, ilmenite, staurolite, plagioclase ± kyanite. The greenschist retrogradation that took place during D3 is marked by the development of chlorite, sericite and new white mica, margarite, green biotite, epidote, albite-rich plagioclase and goethite.

By analyzing the sequence of mineral associations it clearly appears that the evolution of these rocks is retrograde in T and P, from high temperature–high pressure conditions during D1, to a greenschist retrogradation associated with D3 deformation. The reactions involved during this transformation (a to h) are sliding reactions and therefore thermobarometric calculations and chemical composition of different mineral phases are needed to quantify the P-T path.

Mineral chemistry

Chemical composition of minerals were obtained with the ARL-SEMQ electron microprobe of the

C.N.R.-Centro Studi Alpi Centrali in Milano, utilizing natural silicates and oxides as standards. The accelerating voltage was 15 kV and the sample current 20 nA. The structural formulae were determined with MINSORT (PETRAKAKIS and DIETRICH, 1985) and representative chemical compositions of minerals are listed in table 2. Symbols for minerals are from KRETZ (1983) except symbols for phengite and leucophyllite that are Phe and Lc respectively.

White Mica – White micas were analyzed in different microdomains, for both paragneisses and micaschists, separating white micas growing during D3 deformation from those aligned in S2. A third group is constituted by relic white micas preserved as large porphyroclasts (Fig. 4b) or marking the S1 foliation in microlithons of D2 crenulation cleavage (Fig. 3). All the analyzed micas, except some of the syn-D3 micas, can be defined as phengitic muscovites according to GUIDOTTI (1984). Al^{TOT} ranges from 4.65 to 5.80 p.f.u., while Ti is generally less than 0.08 p.f.u. Paragonite rises up to 30% in the white micas of the micaschists and paragneisses, and the lower paragonite content is shown by the older white micas (Fig. 6). It is evident that Tschermak substitution ($Si^{4+} < 6.6$ p.f.u.) is markedly influenced by the Na/(Na + K) ratio and this influence ceases for Pg values lower than 10%. This increment of

Pg content from D1-white micas to D3-white micas is coherent with a decrease in T and P conditions according to GUIDOTTI (1984) and THOMPSON (1976).

Biotite – In the FOSTER (1960) classification diagram the biotites from paragneisses lie in the Mg-biotite field, whereas biotites from micaschists partly invade the Fe-biotite field. In paragneisses the Ti content p.f.u. ranges from 0.09 to 0.21 with $Al^{VI} > 0.85$. X_{Mg} varies between 0.52 and 0.62. For micaschists generally $0.07 < Ti(p.f.u.) < 0.22$ with $Al^{VI} > 0.85$. In this case X_{Mg} ranges from 0.38 to 0.58. The compositional variations of both biotite groups are weak, nevertheless the Ti and Al^{VI} contents decrease in younger biotites.

Staurolite – In both lithologies staurolites have an $X_{Fe} = Fe/(Fe + Mg)$ ranging from 0.79 to 0.83 and a Mn content up to 0.03 p.f.u. They show a compositional zoning in Zn from 0.19 to 0.44 p.f.u. from cores to rims. In response to this variation a weak zoning of Fe and Mg, and a Si change occur.

Plagioclase – The chemical composition of plagioclase in the paragneisses varies as a function of its microstructural position. The plagioclase syn-kinematic with D3 is an albite-rich plagioclase, whereas the syn-D2 plagioclase is oligoclase up to andesine ($An \geq 40$). Pre-D2 grains, enclosed in garnet, show a similarly high An content. In mi-
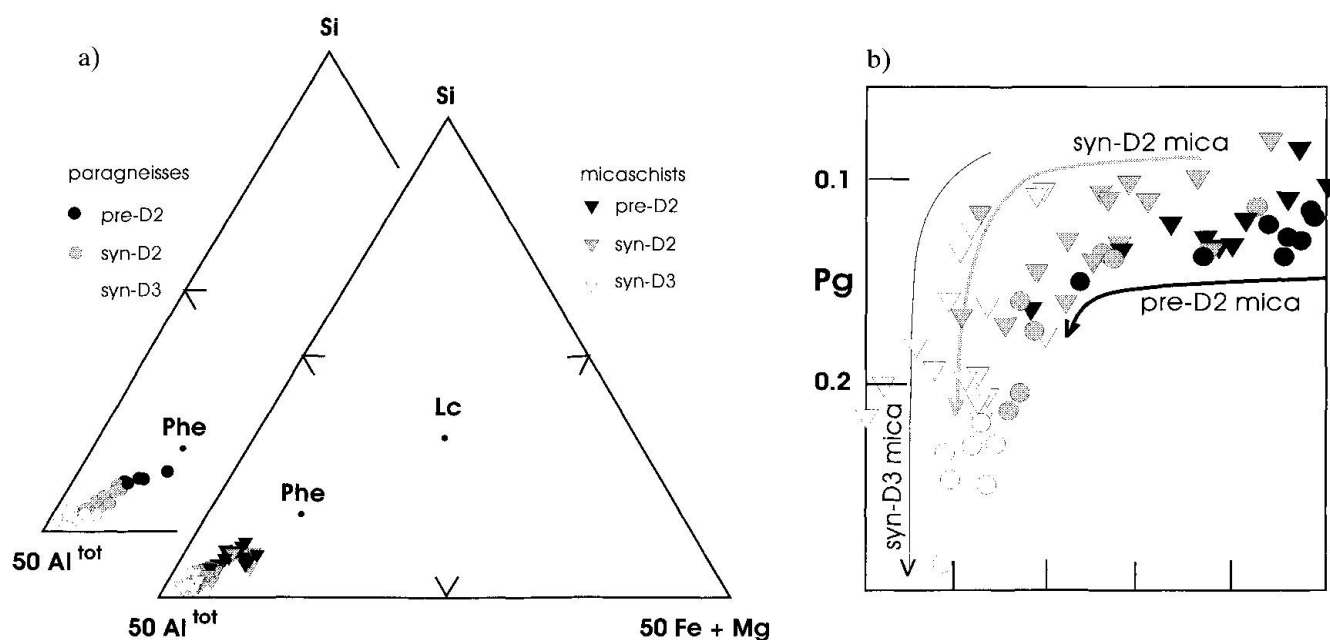

Fig. 6 (a) Classification diagram for phengitic muscovites (MASSONNE and SCHREYER, 1987). Phe = phengite; Lc = leucophyllite. In spite of paragonite influence on the Tschermak substitution the white micas are enriched in celadonite showing a trend from microstructurally younger (syn-D3) to older ones (pre-D2). This evolutionary trend is well represented in the Pg vs Si diagram (b).

Tab. 2 Representative analyses of white mica, biotite, garnet, staurolite and plagioclase of micaschists (msc) and paragneisses (pgn) (stoichiometric ratios of elements based on 22 O for white mica and biotite, 12 for garnet, 8 for plagioclase, 46 for staurolite, 28 for chlorite and 3 for ilmenite).

white mica

	msc pre-D2	msc pre-D2	msc syn-D2	msc syn-D3	pgn pre-D2	pgn syn-D2	pgn syn-D2	pgn syn-D3	pgn syn-D3
SiO_2	50.25	50.47	48.33	47.08	50.01	48.17	47.04	46.57	46.97
TiO_2	0.62	0.62	0.65	0.52	0.72	0.69	0.72	0.63	0.50
Al_2O_3	32.19	30.97	32.68	36.16	28.49	29.45	32.14	35.53	35.18
FeO	1.07	1.47	1.44	0.84	3.79	3.31	3.09	0.98	0.78
MnO	0.02	0.00	0.02	0.02	0.03	0.05	0.03	0.00	0.00
MgO	1.50	2.21	1.86	0.75	2.24	1.97	1.20	0.92	0.85
CaO	0.00	0.00	0.00	0.00	0.00	0.00	0.00	0.00	0.00
Na_2O	0.69	0.81	1.03	2.22	0.46	0.72	0.61	1.25	1.78
K_2O	9.79	9.64	9.82	7.86	10.17	9.90	9.90	9.39	8.30
Total	96.13	96.19	95.83	95.45	95.91	94.26	94.73	95.27	94.36
Si	6.57	6.61	6.38	6.17	6.67	6.53	6.34	6.16	6.23
Al^{IV}	1.43	1.39	1.62	1.83	1.33	1.47	1.66	1.84	1.77
Al^{VI}	3.52	3.38	3.46	3.76	3.15	3.24	3.44	3.70	3.73
Ti	0.06	0.06	0.06	0.05	0.07	0.07	0.07	0.06	0.05
Fe	0.12	0.16	0.15	0.09	0.42	0.38	0.35	0.11	0.09
Mn	0.00	0.00	0.00	0.00	0.00	0.01	0.00	0.00	0.00
Mg	0.29	0.43	0.36	0.15	0.45	0.40	0.24	0.18	0.17
Ca	0.00	0.00	0.00	0.00	0.00	0.00	0.00	0.00	0.00
Na	0.18	0.21	0.27	0.56	0.12	0.19	0.16	0.32	0.46
K	1.63	1.61	1.65	1.31	1.73	1.71	1.70	1.59	1.41
X_{Mg}	0.71	0.73	0.69	0.61	0.51	0.52	0.41	0.63	0.66
Pg	0.10	0.11	0.14	0.30	0.06	0.10	0.09	0.17	0.25
Mu + Ce	0.90	0.89	0.86	0.70	0.94	0.90	0.91	0.83	0.75

biotite

	msc pre-D2	msc pre-D2	msc syn-D2	pgn pre-D2	pgn pre-D2	pgn syn-D2	pgn syn-D2
SiO_2	35.34	38.12	35.78	36.72	36.95	36.85	37.46
TiO_2	2.68	2.01	0.81	1.86	1.90	1.43	1.45
Al_2O_3	18.46	18.55	20.39	19.62	19.61	20.06	19.94
FeO	17.07	17.10	16.90	14.68	15.99	16.97	16.25
MnO	0.00	0.01	0.00	0.00	0.00	0.07	0.05
MgO	11.38	11.49	11.32	12.69	11.88	11.33	11.06
Na_2O	0.23	0.34	0.25	0.33	0.26	0.35	0.28
K_2O	9.80	8.27	9.55	8.88	9.44	8.90	8.71
Total	94.96	95.89	95.00	94.78	96.03	95.96	95.20
Si	5.36	5.63	5.39	5.45	5.46	5.46	5.56
Al^{IV}	2.64	2.38	2.62	2.55	2.54	2.54	2.44
Al^{VI}	0.66	0.85	1.00	0.89	0.88	0.96	1.04
Ti	0.31	0.22	0.09	0.21	0.21	0.16	0.16
Fe	2.17	2.11	2.13	1.82	1.98	2.10	2.02
Mn	0.00	0.00	0.00	0.00	0.00	0.01	0.01
Mg	2.57	2.53	2.54	2.81	2.62	2.50	2.45
Na	0.07	0.10	0.07	0.10	0.08	0.10	0.08
K	1.90	1.56	1.83	1.68	1.78	1.68	1.65
X_{Mg}	0.54	0.55	0.54	0.61	0.57	0.54	0.55

staurolite

	core	core	rim	rim
SiO_2	28.41	27.86	28.21	28.33
TiO_2	0.71	0.82	0.53	0.50
Al_2O_3	53.84	54.31	53.75	52.66
FeO	11.83	11.67	12.40	12.88
MnO	0.04	0.07	0.12	0.07
ZnO	2.17	2.07	1.17	0.92
MgO	1.69	1.56	1.70	1.84
Total	98.69	98.37	97.91	97.25
Si	7.82	7.69	7.81	7.91
Ti	0.15	0.17	0.11	0.11
Al	17.47	17.67	17.54	17.32
Fe	2.72	2.69	2.87	3.01
Mn	0.01	0.02	0.03	0.02
Zn	0.44	0.42	0.24	0.19
Mg	0.69	0.64	0.70	0.77

plagioclase

	msc syn-D2	pgn syn-D2	pgn syn-D3
SiO_2	62.46	56.62	67.18
TiO_2	0.01	0.00	0.00
Al_2O_3	24.66	27.25	20.68
FeO	0.13	0.17	0.11
MgO	0.00	0.03	0.01
CaO	5.69	9.03	1.32
Na_2O	8.63	6.42	10.81
K_2O	0.05	0.07	0.16
Total	101.63	99.59	100.27
Si	2.73	2.55	2.94
Al	1.27	1.45	1.07
Ti	0.00	0.00	0.00
Fe	0.01	0.01	0.00
Mg	0.00	0.00	0.00
Ca	0.27	0.44	0.06
Na	0.73	0.56	0.92
K	0.00	0.00	0.01
An	0.27	0.44	0.06
Ab	0.73	0.56	0.93
Or	0.00	0.00	0.01

garnet

	msc core	msc rim	pgn core	pgn rim
SiO_2	37.57	37.18	37.62	37.88
TiO_2	0.10	0.00	0.15	0.11
Al_2O_3	21.54	21.93	20.62	20.74
FeO	28.92	31.41	27.67	31.38
MnO	0.76	0.79	3.76	0.17
MgO	2.69	3.22	1.25	2.76
CaO	7.92	5.26	9.38	7.68
Total	99.50	99.80	100.45	100.72
Si	2.99	2.96	3.00	3.00
Al^{IV}	0.01	0.04	0.00	0.00
Al^{VI}	2.01	2.03	1.94	1.93
Ti	0.01	0.00	0.01	0.01
Fe^{3+}	0.00	0.00	0.05	0.06
Fe^{2+}	1.93	2.09	1.79	2.01
Mn	0.05	0.05	0.25	0.01
Mg	0.32	0.38	0.15	0.33
Ca	0.68	0.45	0.80	0.65
Alm	0.70	0.70	0.60	0.67
Sps	0.02	0.02	0.09	0.00
Pyr	0.11	0.13	0.05	0.11
Grs	0.22	0.15	0.24	0.18
Anr	0.00	0.00	0.03	0.03

chlorite

	msc	pgn
SiO_2	25.76	28.51
TiO_2	0.06	0.04
Al_2O_3	22.71	20.63
FeO	23.52	21.51
MnO	0.07	0.19
MgO	16.28	16.35
CaO	0.04	0.06
Na_2O	0.03	0.03
K_2O	0.00	0.07
Total	88.47	87.39
Si	5.31	5.86
Al^{IV}	2.69	2.14
Al^{VI}	2.83	2.86
Ti	0.01	0.01
Fe	4.05	3.70
Mn	0.01	0.03
Mg	5.00	5.01
Ca	0.01	0.01
Na	0.01	0.01
K	0.00	0.02
X_{Mg}	0.55	0.57

ilmenite

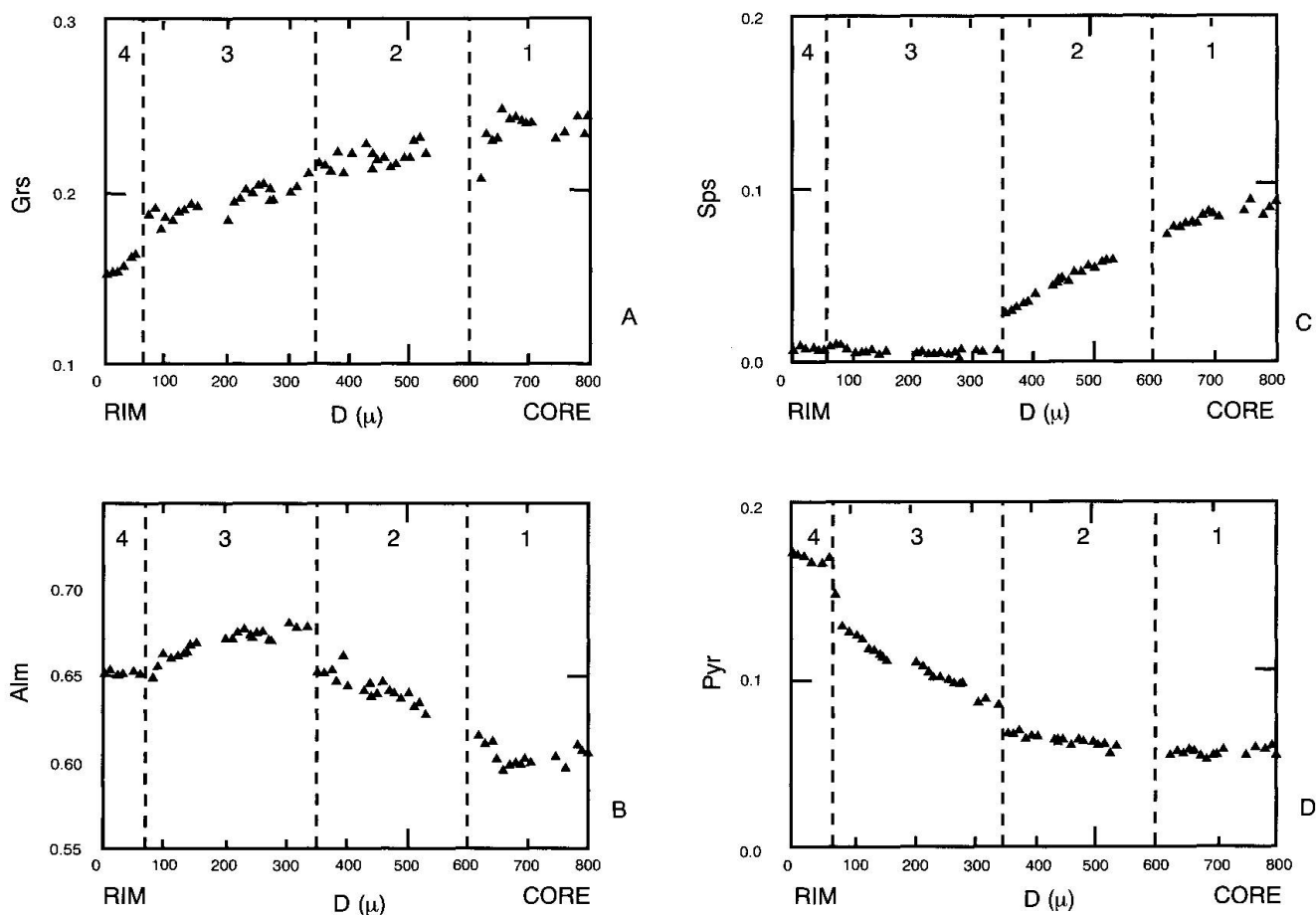|	msc	pgn
SiO_2	0.00	0.06
TiO_2	47.97	49.30
Al_2O_3	0.02	0.01
FeO	50.05	47.19
MnO	0.84	2.92
ZnO	0.00	0.11
MgO	0.00	0.08
CaO	0.01	0.02
Total	98.90	99.70
Si	0.00	0.00
Al	0.00	0.00
Ti	0.92	0.94
Fe^{3+}	0.16	0.13
Fe^{2+}	0.90	0.87
Mn	0.02	0.06
Zn	0.00	0.00
Mg	0.00	0.00
Ca	0.00	0.00
X_{Fe}	0.98	0.93

Fig. 7 Zoning profile of a paragneiss garnet in distance (D = μm) vs chemical composition from rim (0.0 μm) to core (800 μm). GRS = grossular; ALM = almandine; PYR = pyrope; SPS = spessartine.

caschists the An content is 18–27%, and the plagioclase porphyroblasts show a compositional zoning with a decrease of An from core to rim.

Garnet – In paragneisses garnets are almandine-spessartine-grossular-pyrope solid solutions, with 57–69% almandine, 5–19% pyrope, 11–25% grossular and with up to 12% spessartine. Rarely andradite occurs rising up to 5%. For some of these garnets the analyses were made along traverses, from cores to rims of the grains, at 10 μm intervals with a beam diameter of 10 μm to obtain a continuous zoning profile (Fig. 7). The trends of the chemical variation from core to rim of grains define (Fig. 8) a first growth stage characterized by a Mn decrease with a quite constant Ca/Fe + Mg ratio, followed by a decrease of both Ca and Mn and finally by a strong decrease in Ca with a constant Mn/Fe + Mg ratio. During the first stage of growth garnet shows prevailing enrichment of Fe at the expenses of Mg (Fig. 8), with a progressive enrichment in Mg during the subsequent stages. Compositions of garnet rims developing at the end of D2 deformation plot in the

dashed field; the shaded field represents chemical compositions of garnet rims in contact with syn-D2 biotites. In this latter case the Mg-enrichment is probably related to the Fe^{2+}–Mg exchange between coexisting garnet and biotite. In micaschists zoning profiles of garnets (Fig. 8) show similar trends of chemical variations, with the exception of spessartine content that is significantly lower (max. 3%).

The zoning patterns of garnet can be related to the metamorphic reactions deduced by the microstructural analysis. Generally these garnets show a homogeneous central sector (stage 1 in Fig. 7) that may be interpreted as due to homogeneization by intracrystalline diffusion related to a high temperature regime (> 650 °C; e.g. THOMPSON et al., 1977; TRACY et al., 1976) or to the persistence over a long span of time of the same P-T conditions. The continuous decrease of Ca (stage 2 and 3 in Fig. 7) is compatible with the occurrence of the continuous reaction (b). The pyrope increment at the expenses of almandine (stage 3 in Fig. 7) is well correlated with the growth of a
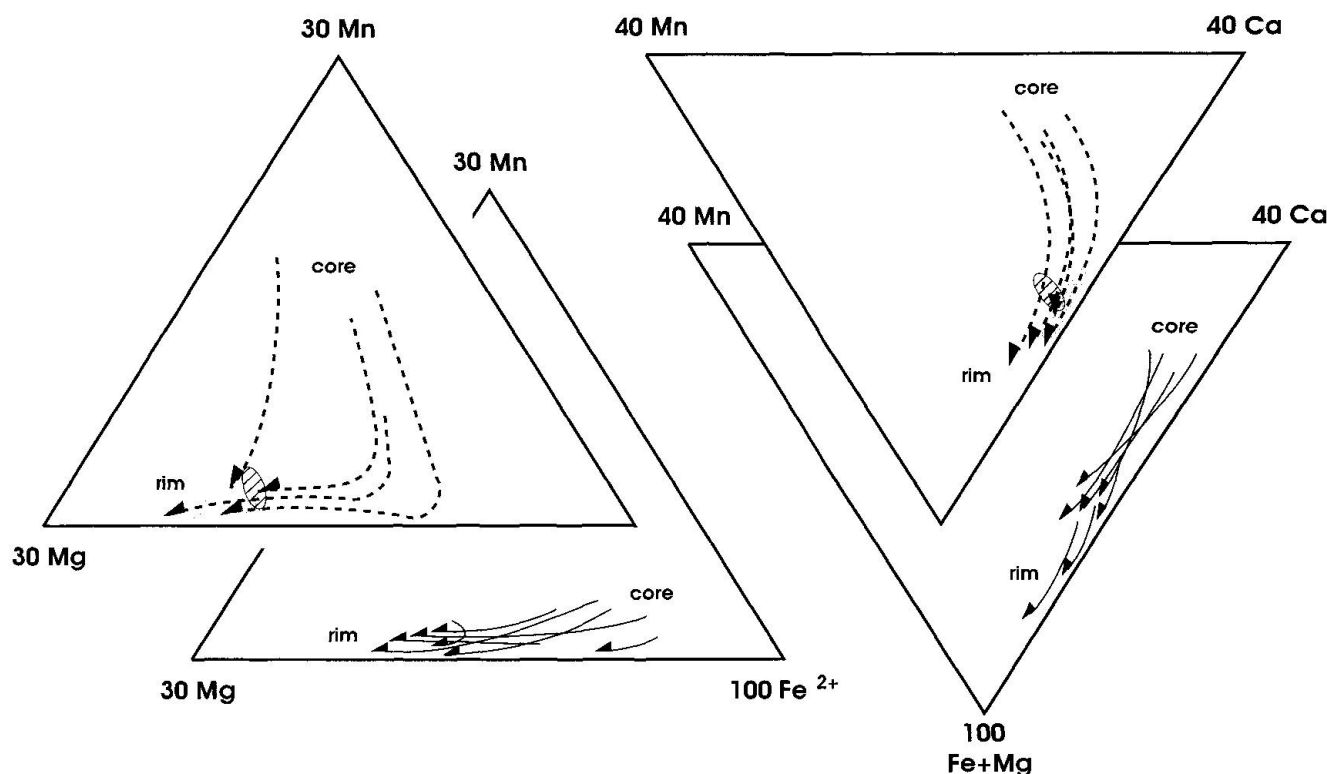
Fig. 8 Zoning trends of micaschists garnets (solid lines) and of paragneisses garnets (dashed lines). The dashed area represents garnet rims newly formed during D2 final stages of deformation.

Fe-rich mineral phase as staurolite (reaction c) or with Fe–Mg partitioning with other iron-magnesium-bearing mineral phases.

Ilmenite – Ilmenite is characterized by a Mn content comprised between 0.02 and 0.06 p.f.u. with traces of Zn and Mg.

Chlorite – Chlorites from micaschists have an X_{Fe} = 0.45 and 5.3 < Si < 5.7 p.f.u.: on the HEY (1954) diagram they plot in the ripidolites field; chlorites from paragneisses are characterized by a lower iron content ($0.37 < X_{Fe} < 0.45$) and higher Si (from 5.7 to 6.1 p.f.u.): they plot in the pycnochlorites field.

The chemical evolution of different mineral phases concordantly suggest a retrograde P-T evolution in agreement with the microstructural observations. Garnet seems to be the only mineral that still records earlier stages of the metamorphic evolution; actually it shows cores with homogeneous composition over an interval > 200 μm.

P-T estimates

In order to quantify the physical conditions of different metamorphic stages related to different steps of the deformational history (Tab. 3) garnet-biotite and garnet-staurolite Fe–Mg cationic exchanges were utilized to obtain T values and GRAIL (Garnet-Rutile-Aluminum Silicate-Ilmenite-quartz) and garnet-plagioclase barometers to define P values during the two earlier deformation episodes that developed under high T-high P conditions.

For the greenschist retrogradation that took place during D3 the available experimental reaction curves were utilized for defining the P-T range.

Finally, with the purpose of better constraining the P evolution, the variation in Si^{4+} content was studied in phengitic micas associated to metagranitoids cropping out in the Texel Gruppe, where the limiting assemblage K-feldspar, biotite, phengite and quartz occurs. They were separated in three groups on the base of their positions with respect to successive foliations, adopting the same criteria utilized for the microstructural analysis in metapelites that is pre-D2, syn-D2 and syn-D3 white micas.

The sites suitable for chemical analyses with thermobarometric aims were selected by looking at the timing of mineral growth with respect to the successive phases of deformation and also at sites where different deformation mechanisms were

Tab. 3   Representative mineral composition and related thermobarometric estimates for micaschists (msc) and paragneisses (pgn). Si^{4+} content of white mica (WM) is considered for metagranitoids (mgr) only.

Table 3: Representative mineral composition and related thermobarometric estimates for micaschists (msc) and paragneisses (pgn). Si 4+ content of white mica (WM) is considered for metagranitoids (mgr) only.

lithology	stage	Bt	Grt				St	Ilm	Plg	Phe	FS	PL	Pr	B	G	MS
		XMg	XMg	XCa	XFe	XMn	XMg	XFe	XAn	Si4+ (p.f.u.)	T(°C)	T(°C)	T(°C)	P(GPa); T*(°C)	P(GPa); T*(°C)	P(GPa); T*(°C)
msc	pre-D2	0.453-0.476	0.149-0.168	0.012-0.152		0.006-0.021					688 3σ=73	643 3σ=30				
pgn	pre-D2	0.588-0.594	0.201-0.214	0.177-0.198		0.014-0.032					"	"				
msc	pre-D2				0.805-0.838			0.969-0.980						0.9-1.0; 640-680		
pgn	pre-D2				0.614-0.688			0.932-0.943						"		
msc	syn-D2	0.500-0.542	0.119-0.133	0.136-0.200		0.004-0.028					551 3σ=71	580 3σ=40				
pgn	syn-D2	0.574-0.611	0.137-0.172	0.117-0.168		0.006-0.020					"	"				
msc	syn-D2		0.153-0.165				0.187-0.203						~570			
pgn	syn-D2		0.149-0.171				0.195-0.204						"			
msc	syn-D2		0.209-0.219						0.252-0.266						0.6-0.75; 550-580	
pgn	syn-D2		0.204-0.253						0.366-0.435						"	
mgr	pre-D2									3.30±0.05						~1.0; 640-680
mgr	syn-D2									3.20±0.05						~0.7; 550-580
mgr	syn-D3									3.05±0.05						~0.3; <500

FS = FERRY and SPEAR (1978); PL = PERCHUK and LAVRENT'EVA (1983); Pr = PERCHUK (1969); B = BOHLEN et al. (1983); G = GHENT (1976); MS = MASSONNE and SCHREYER (1987). T* = T imposed for P calculations.
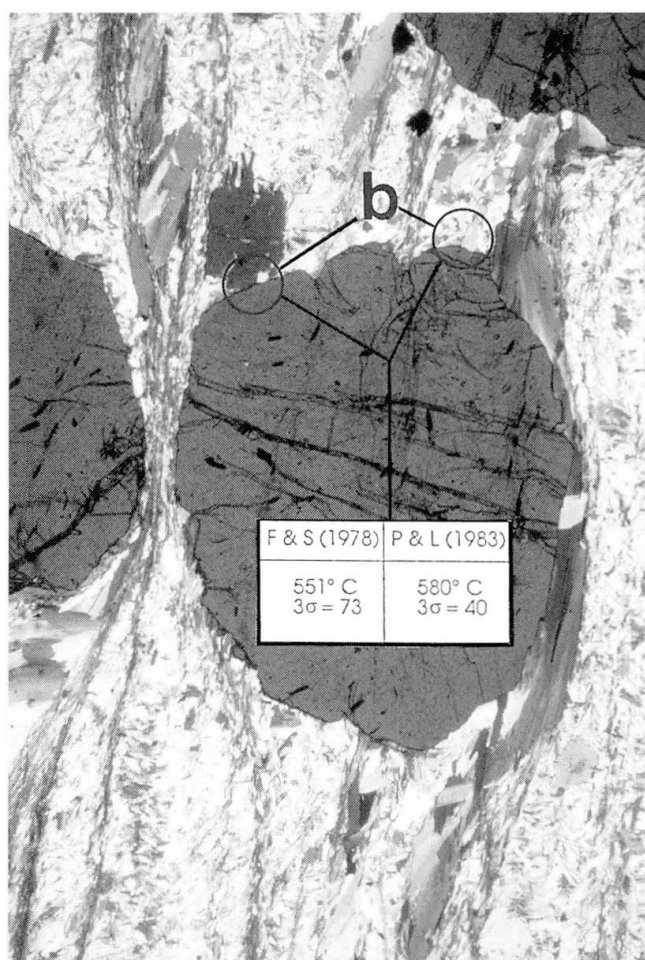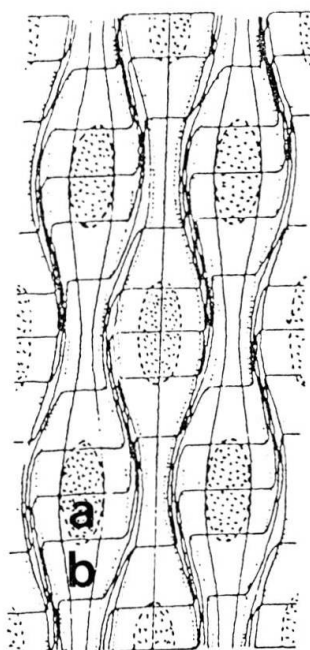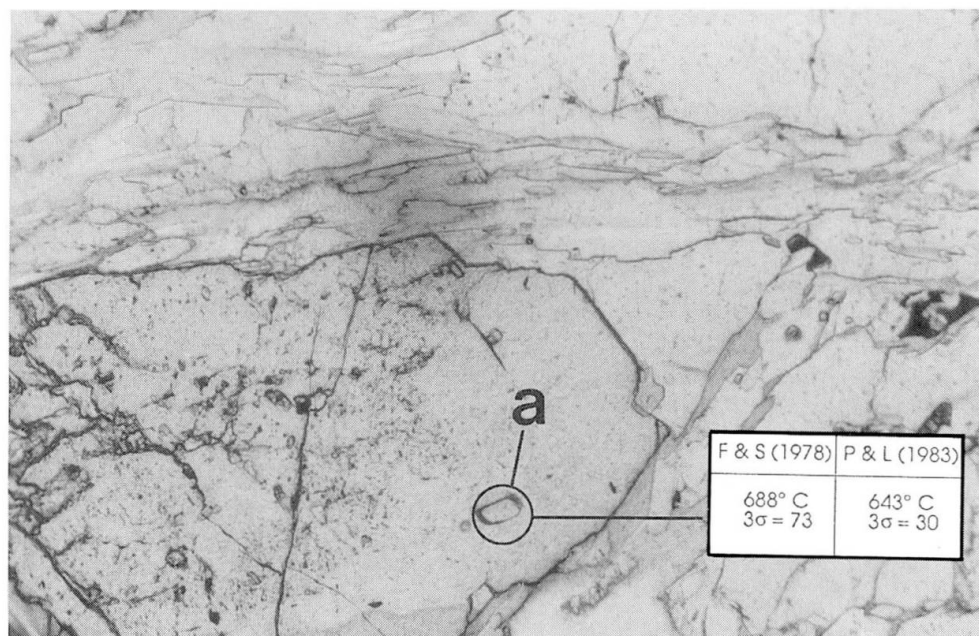
F & S (1978)	P & L (1983)
688° C 3σ = 73	643° C 3σ = 30

F & S (1978)	P & L (1983)
551° C 3σ = 73	580° C 3σ = 40

Fig. 9 Example of armoured inclusion of biotite in garnet (a) representing a microstructural relic preserved in zones where no strain occurs during deformation partitioning (shaded area in the interpretative strain pattern of cleavage formation BELL et al., 1986). T-values obtained in these sites plot in the group of pre-D2 temperatures (Tab. 3). In the sites of prevailing coaxial progressive shortening (b) new mineral growth is facilitated during foliation development: therefore garnet biotite pairs occurring in D2 microlithons were utilized to obtain syn-D2 T-values (Tab. 3).

active during the same deformation event, according to BELL and HAYWARD (1991 and references therein).

Following this model microdomains where strain is scarce or absent (Fig. 9) and preservation of relic equilibria is possible, as in the armoured inclusions of garnet, have been distinguished from sites in which mineral growth is contemporaneous to the foliation development, as in microlithons (SPALLA, 1989a).

For the garnet-biotite equilibrium the FERRY and SPEAR (1978) and the PERCHUK and LAVRENT'EVA (1983) calibrations (FS and PL respectively in Tab. 3) were utilized, but the PL calibration was chosen as reference because it takes into account also strong variations in N_{Al}^{Bi} and it is calibrated for higher pressure than the FS thermometer. For the pre-D2 garnet-biotite pairs the obtained T values range from 640 and 680 °C. For the garnet-biotite pairs lying in the D2 microlithons the calculated values vary between 550 and 580 °C. These results fit well with the TiAl^{VI} content of biotites, that show only weak variations between pre-D2 and syn-D2 biotites and suggest a range between 500 and 650 °C according to SCHREURS (1985). It must be noted that for biotites with higher values of X_{Mg} these represent minimum temperatures, because X_{Mg} values of about 0.6 or more, inhibit Ti substitution (GUIDOTTI et al., 1977).

The partitioning of Fe and Mg between syn-D2 staurolite and garnet (PERCHUK, 1969) gives temperature of ~570 °C (P in Tab. 3).

The garnet-rutile-aluminum silicate-ilmenite-quartz (GRAIL) equilibrium (BOHLEN et al., 1983), here interpreted as predating D2 deformation, yields a pressure of 0.9–1.0 GPa. Pressure values of 0.6–0.75 GPa were obtained for the garnet-kyanite-quartz-plagioclase equilibrium (syn-D2) utilizing GHENT's (1976) calibration.

Solution models of GANGULY and SAXENA (1984) and NEWTON and HASELTON (1981)[1] were adopted for determining almandine-grossular and anorthite activities in garnet and plagioclase, respectively; ilmenite was considered as an ideal solid solution.

According to GOLDSMITH (1982) the compositional trends of plagioclase are compatible with a temperature decrease; the more anorthitic plagioclase (An > 40) indicates T > 500 °C for P > 0.6 GPa.

The greenschist retrogradation, associated with D3 deformation, took place at T < 500 °C and P < 0.4 GPa as suggested by reactions (d) and (e) (Fig. 10).

The three groups of white micas in metagranitoids, selected with microstructural criteria, show different values of Si^{4+} p.f.u. (Tab. 3) giving P values of ~1.0 GPa (640 < T < 680 °C) for pre-D2 micas, of ~0.7 GPa (550 < T < 580 °C) for syn-D2 micas and of ~0.3 GPa (T < 500 °C) for syn-D3 micas, the method of MASSONNE and SCHREYER (1987) being used.

Conclusive remarks

Plotting the P-T values relative to each group of structures, we obtain a *P-T-relative time of deformation path* (Fig. 10) in which the resulting P-T boxes are relatively small. These results show clearly, that the T and P values would be considerably scattered without the assistance of microstructural analysis. Garnet biotite pairs for example, yield temperatures between 550 and 680 °C or more (SPALLA, 1989a).

The P values obtained from the Si^{4+} content of white mica result also in an undifferentiated large group with a pressure interval of 0.3–1.0 GPa. It must be underlined that not only the independent thermometers and barometers used here, but also the chemical variation of mineral phases and the qualitative P-T evolution, deduced by the sequence of experimental sliding reactions, give consistent results.

Finally the *P-T-relative time of deformation* path established represents a good constraint to relating this tectono-metamorphic evolution with that deduced in surrounding areas. For attributing geological significance to these data the wealth of radiometric ages available in this part of the Alpine chain can be taken into consideration. An AMA (Alpine Mica Age) region has been identified, which encloses the Texel Gruppe metapelites and eclogites considered of eo-Alpine age by HOINKES et al. (1991). The eclogites represent lenticular relics embodied within the amphibolite facies foliation marked by Alpine biotite and white mica (THOENI and HOINKES, 1987). This Alpine foliation corresponds to the S2 foliation in the Texel Gruppe. Definitely two metamorphic signatures, namely the eclogitic (P = 1.1–1.2 GPa, T = 500–550 °C) and the D1 stage (P = 0.9–1.0

---

[1] Almandine: $a_{alm} = \{X_{Fe} \exp [[200 (X_{Mg})^2 + 4600 X_{Fe} + (X_{Ca})^2 (4083 - 1.5T - 7866 X_{Fe}) + X_{Mg}X_{Ca} [943 - 1633 X_{Fe} - 3047 (X_{Mg} - X_{Ca}) - 4640 (1-2 X_{Fe})] + X_{Ca}X_{Mn} [2117 - 1.5T - 3933X_{Fe} + 1917 (1-2 X_{Fe})] + X_{Mg}X_{Mn} [-1650 + 2300 X_{Fe} - 1150 (1-2 X_{Fe})] + 3048 (X_{Mg}X_{Ca}X_{Mn})] / RT\}^3$ (GANGULY and SAXENA, 1984); Grossular: $a_{grs} = \{X_{Ca} \exp [[(13807-6.3T)((X_{Mg})^2 + (X_{Mg}X_{Fe}))]/RT]\}^3$ (NEWTON and HASELTON, 1981); Anorthite: $a_{an} = 0.25 [X_{Ca} (1 + X_{Ca})^2] \exp \{(1-X_{Ca})^2 [1032 + 4726 X_{Ca}]\}$ (NEWTON and HASELTON, 1981).
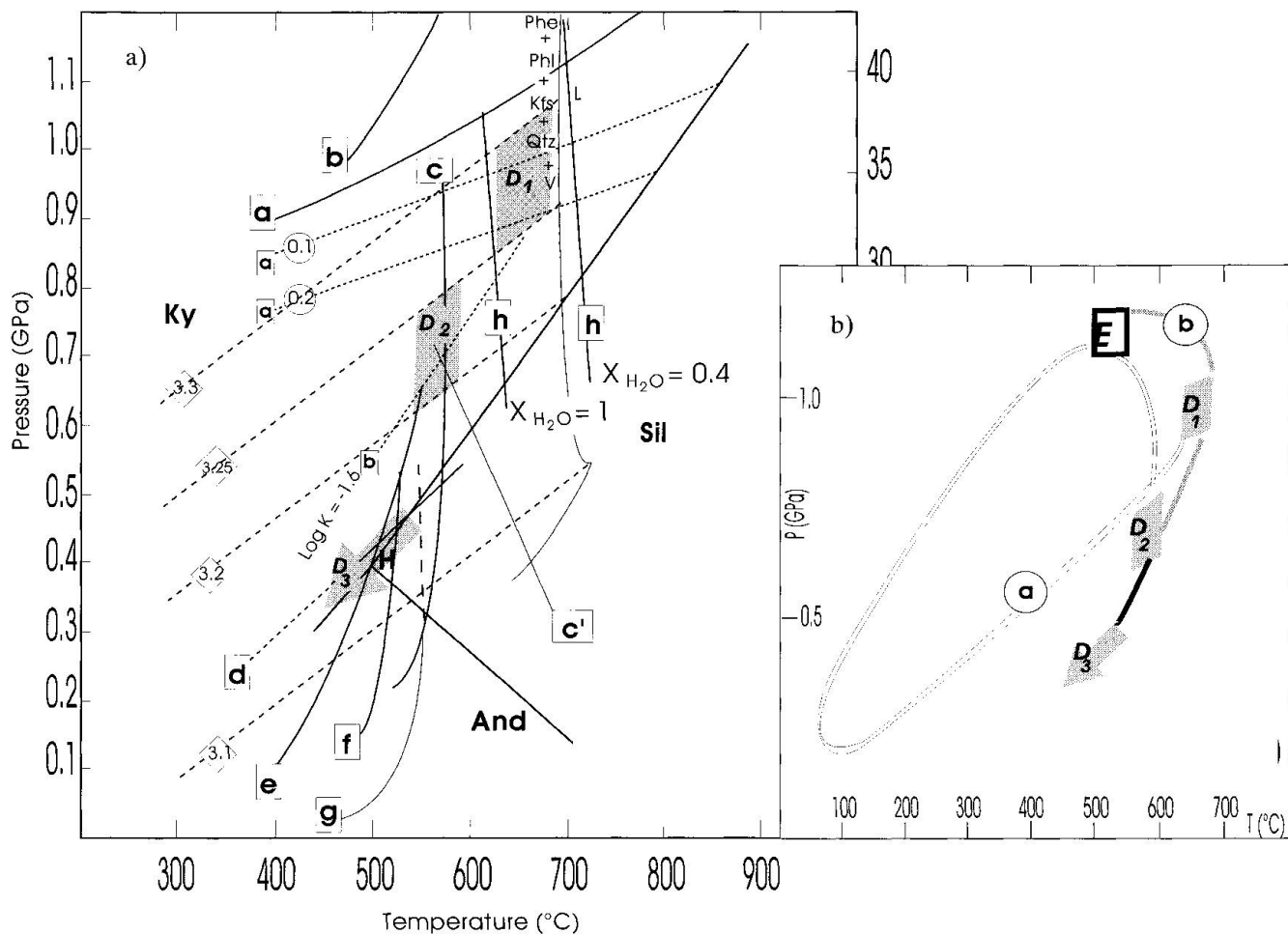
Fig. 10 (a) P-T path of the Texel metapelites; D1, D2 and D3 represent P-T conditions of assemblages during successive generation of structures. Aluminum silicate triple point: H = Holdaway (1971); Phe + Phl + Kfs + Qtz + V = L and isopleths of Si^{4+} content in phengites are taken from Massonne and Schreyer (1987). All the other reactions are labelled from a to h as in the text. For reactions a and b significant Log K are represented. (b) Possible paths (a and b) between the eclogitic (= E), D1, D2 and D3 tectonometamorphic steps. D2-D3 segment represents the final stage of uplift in both paths.

GPa, T = 640–680 °C), are therefore ascertained before the D2 (P = 0.6–0.75 GPa, T = 550–580 °C) Alpine deformation, but their relative age is debatable in the absence of continuous structural informations. Two possible interpretations can therefore be proposed:

1) The age of the D1 tectonometamorphic event is pre-Alpine and related to the Variscan cycle, and it is followed by a transition to eclogitic conditions during Alpine time. In this case D1 should be followed by an uplift and a subsequent underthrusting before the Alpine eclogitic stage (path a in Fig. 10b). Metamorphic signatures of the exhumation and subduction trajectories would therefore be preserved, embodied in the S2 foliation (i.e. the D1 and eclogitic stages).

2) D1 postdates the eclogitic stage (path b in Fig. 10b) and is therefore Alpine. Consequently

D1 should correspond to a stage of thermal relaxation after continental collision and subduction related eclogite formation, before uplift (D2 + D3 stages). In any case it can be concluded that, disregarding the pre- or post-eclogitic age of D1, the D2 to D3 P-T path represents the uplift of this portion of Upper Austroalpine crust from a level deeper than 30 km during Alpine time.

Quaternaria (C.N.R., Milano) for installation and operation of the electron microprobe laboratory. Mr S. Uggeri kindly provided the polished thin sections. This work is dedicated to the memory of Ugo Pognante to whom I am indebted as a student of his early times at the Institute of Petrography in Torino.

References

ANGENHEISTER, G., BÖGEL, H., GEBRANDE, H., GIESE, P., SCHMIDT-THOMÉ, P. and ZEIL, W. (1972): Recent investigations of surficial and deeper crustal structures of the Eastern and Southern Alps. Geol. Rdsch. 61, 349–395.

BELL, T.H. (1986): Foliation development and refraction in metamorphic rocks: reactivation of earlier foliations and decrenulation due to shifting patterns of deformation partitioning. J. Metamorphic Geol. 4, 421–444.

BELL, T.H. and HAYWARD, N. (1991): Episodic metamorphic reactions during orogenesis: the control of deformation partitioning on reaction sites and reaction duration. J. Metamorphic Geol. 9, 619–640.

BELL, T.H. and RUBENACH, M.J. (1983): Sequential porphyroblast growth and crenulation cleavage development during progressive deformation. Tectonophysics 92, 171–194.

BELL, T.H., RUBENACH, M.J. and FLEMING, P.D. (1986): Porphyroblast nucleation, growth and dissolution in regional metamorphic rocks as a function of deformation partitioning during foliation development. J. Metamorphic Geol. 4, 37–67.

BOHLEN, S.R., WALL, V.J. and BOETTCHER, A.L. (1983): Experimental investigations and geological applications of equilibria in the system $FeO-TiO_2-Al_2O_3-SiO_2-H_2O$. Amer. Mineral. 68, 1049–1058.

CARMICHAEL, D.M. (1978): Metamorphic bathozones and bathograds: a measure of the depth of post-metamorphic uplift and erosion on the regional scale. Amer. J. Sci. 278, 769–797.

CHATTERJEE, N.D. (1976): Margarite stability and compatibility relations in the system $CaO-Al_2O_3-SiO_2-H_2O$ as a pressure-temperature indicator. Amer. Mineral. 61, 699–709.

CIMMINO, F. and MESSIGA, B. (1979): I calcescisti del Gruppo di Voltri (Liguria occidentale): le variazioni composizionali delle miche bianche in rapporto all'evoluzione tettonico-metamorfica alpina. Ofioliti 4, 269–294.

FERGUSON, C.C. and HARTE, B. (1975): Textural patterns at porphyroblast margins and their use in determining the time relations of deformation and crystallization. Geol. Mag. 112, 467–480.

FERRY, J.M. and SPEAR, F.S. (1978): Experimental calibration of the partitioning of Fe and Mg between biotite and garnet. Contrib. Mineral. Petrol. 66, 113–117.

FOSTER, M.D. (1960): Interpretation of the composition of trioctahedral micas. U.S. Geol. Surv. Prof. Paper 575, C17–C22.

FRANK, W. (1987): Evolution of the Austroalpine elements in the Cretaceous. In: FLÜGEL, H.W. and FAUPL, P. (eds), Geodynamics of the Eastern Alps, Deuticke-Wien, 379–403.

FRANK, W., HOINKES, G., PURTSCHELLER, F. and THOENI, M. (1987): The Austroalpine units west of the Hohe Tauern: the Ötztal-Stubai complex as an example for the eo-Alpine metamorphic evolution. In:

FLÜGEL, H.W. and FAUPL, P. (eds): Geodynamics of the Eastern Alps, Deuticke-Wien, 379–403.

FRISCH, W. (1979): Tectonic progradation and plate tectonic evolution of the Alps. Tectonophysics 60, 121–139.

GANGULY, J. and SAXENA, S.K. (1984): Mixing properties of aluminosilicate garnets: constraints from natural and experimental data, and applications to geothermo-barometry. Amer. Mineral. 69, 88–97.

GHENT, E. (1976): Plagioclase-garnet-Al_2SiO_5-quartz: a potential geobarometer and geothermometer. J. Petrol. 61, 710–714.

GOLDSMITH, J.R. (1982): Plagioclase stability at elevated temperatures and water pressures. Amer. Mineral. 67, 653–675.

GOSSO, G. (1977): Metamorphic evolution and fold history in the eclogite micaschists of the upper Gressoney valley (Sesia-Lanzo zone, Western Alps). Rend. Soc. It. Mineral. Petrol. 33, 389–407.

GUIDOTTI, C.V. (1984): Micas in metamorphic rocks. In: BAILEY, S.W. (eds), Micas, Amer. Mineral. Reviews in Mineralogy 13, 357–468.

GUIDOTTI, C.V., CHENEY, J.T. and GUGGENHEIM, S. (1977): Distribution of Ti between coexisting muscovite and biotite in pelitic schists from northwestern Maine. Amer. Mineral. 62, 438–448.

HALL, W.D.M. (1972): The structural and metamorphic history of the lower pennine nappes, Valle di Bosco, Ticino, Switzerland. Ph.D. Thesis Imperial Coll. London.

HAYS, J.F. (1967): Lime-alumina-silica. Carnegie Inst. Wash. Yearb. 65, 234–239.

HEY, M.H. (1954): A new review of the chlorites. Miner. Mag. 30, 277 pp.

HIGGINS, A.K. (1964): The structural and metamorphic geology of the area between Nufenenpass and Basodino, Tessin, Switzerland. Ph.D. Thesis Imperial Coll. London.

HIRSCHBERG, A. and WINKLER, H.C.F. (1968): Stability relations between cordierite, chlorite and almandine during metamorphism. Contrib. Mineral. Petrol. 18, 17–42.

HOBBS, B.E., MEANS, W.D. and WILLIAMS, P.F. (1976): An outline of structural geology. Wiley – New York, 571 pp.

HOINKES, G., KOSTNER, A. and THÖNI, M. (1991): Petrologic Constraints for Eo-Alpine Eclogite Facies Metamorphism in the Austroalpine Ötztal Basement. Mineralogy and Petrology 43, 237–254.

HOSCHEK, G. (1969): The stability of staurolite and chloritoid and their significance in metamorphism of pelitic rocks. Contrib. Mineral. Petrol. 22, 208–232.

HSÜ, L.C. (1968): Selected phase relationships in the system Al–Mn–Fe–Si–O–H: a model for garnet equilibria. J. Petrol. 9, 49–83.

HUBER, M., RAMSAY, J.G. and SIMPSON, C. (1980): Deformation in the Maggia and Antigorio nappes, Lepontine Alps. Eclogae geol. Helv. 73, 593–606.

KRETZ, R. (1983): Symbols for rock-forming minerals. Amer. Mineral. 68, 277–279.

LARDEAUX, J.M., GOSSO, G., KIENAST, J.R. and LOMBARDO, B. (1983): Chemical variations in phengitic micas of successive foliations within the Eclogitic Micaschists complex, Sesia-Lanzo zone (Italy, Western Alps). Bull. Minéral. 106, 673–689.

LARDEAUX, J.M. and SPALLA, M.I. (1990): Tectonic significance of P-T-t paths in metamorphic rocks: examples from ancient and modern orogenic belts. Mem. Soc. Geol. It. 45, 51–69.

MASSONNE, H.J. and SCHREYER, W. (1987): Phengite geobarometry based on the limiting assemblage with

k-feldspar, phlogopite and quartz. Contrib. Mineral. Petrol. 96, 212–224.

MØRK, M.B. (1985): A gabbro to eclogite transition on Flemsoy, Suamore, Western Norway. Chem. Geol. 50, 283–310.

NAGGAR, M.H. and ATHERTON, M.P. (1970): The composition and metamorphic history of some aluminium silicate-bearing rocks from the aureoles of the Donegal granites. J. Petrol. 11, 549–589.

NEWTON, R.C. and HASELTON, H.T. (1981): Thermodynamics of the garnet-plagioclase-Al_2SiO_5-quartz geobarometer. In: Thermodynamics of melts and minerals. Ed. by NEWTON, R.C., NAVROTSKY and WOOD. Springer-Verlag New York, 131–147.

PERCHUK, L.L. (1969): The staurolite-garnet thermometer. Dokl. Acad. Sci. USSR Earth Sci. Sect. 186, 189–191.

PERCHUK, L.L. and LAVRENT'EVA, I.V. (1983): Experimental investigation of exchange equilibria in the system cordierite-garnet-biotite. In: Kinetics and equilibrium in mineral reactions, Ed. by SAXENA, S.K. Springer-Verlag. New York, 199–239.

PETRAKAKIS, K. and DIETRICH, H. (1985): MINSORT: a program for the processing and archiviation of microprobe analyses of silicate and oxide minerals. N. Jb. Mineral. Mh. 8, 379–384.

POLI, S. (1989): Problemi di petrologia ignea e metamorfica nelle metabasiti: un esempio dal basamento Austroalpino. Ph.D. Thesis. University of Milano.

POWELL, C.M. and VERNON, R.H. (1979): Growth and rotation history of garnet porphyroblasts with inclusion spirals. Tectonophysics 54, 25–43.

RAMSAY, J.G. and GRAHAM, R.H. (1970): Strain variation in shear belts. Can. J. Earth Sci. 7, 786–813.

RAO, B.B. and JOHANNES, W. (1979): Further data on the stability of staurolite + quartz and related assemblages. N. Jb. Mineral. 1979, 437–447.

SCHMID, S.M. and HAAS, R. (1989): Transition from near-surface thrusting to intrabasement decollement, Schlinig Thrust, Eastern Alps. Tectonics 8, 697–718.

SCHREURS, J. (1985): Prograde metamorphism of metapelites, garnet-biotite thermometry and prograde changes of biotite chemistry in high grade rocks of West Uusimaa, southwest Finland. Lithos 18, 69–80.

SPALLA, M.I. (1989 a): Percorsi P-T e tempi relativi della deformazione nella crosta Austroalpina dell'Ötztal: l'ortogneiss di Parcines e le sue rocce incassanti. Ph.D. Thesis. University of Milano.

SPALLA, M.I. (1989b): A retrograde P-T path and relative timing of deformation in the Ötztal nappe: an interpretation of the orogenic metamorphism in the Austroalpine crust. Terra Abst. 1, 297.

SPALLA, M.I. (1990a): Polyphased deformation during uplifting of metamorphic rocks: the example of the deformational history of the Texel Gruppe (Central-Western Austroalpine Domain of the Italian Eastern Alps). Mem. Soc. Geol. It. 45, 125–134.

SPALLA, M.I. (1990 b): Structural map of the Upper Spronsertal – Texel Gruppe. Mem. Soc. Geol. It. (45) Roma.

THOENI, M. and HOINKES, G. (1987): The Southern Ötztal Basement: Geochronological and Petrological Consequences of Eo-alpine Metamorphic Overprinting. In: FLÜGEL, H.W. and FAUPL, P. (eds), Geodynamics of the Eastern Alps, Deuticke-Wien, 200–213.

THOMPSON, A.B. (1976): Mineral reactions in pelitic rocks, I. Predictions of P-T-X (Fe–Mg) phase relations. II. Calculation of some P-T-X (Fe–Mg) phase relations. Amer. J. Sci. 276, 201–254.

THOMPSON, A.B., TRACY, R.J., LYTTLE, P. and THOMPSON, J.B.J. (1977): Prograde reactions histories deduced from compositional zonation and mineral inclusions in garnet from the Gassetts schists, Vermont. Amer. J. Sci. 277, 1152–1167.

TRACY, R.J., ROBINSON, P. and THOMPSON, A.B. (1976): Garnet composition and zoning in the determination of temperature and pressure of metamorphism, Central Massachusset. Amer. Mineral. 61, 762–765.

VAN GOOL, J.A.M., KEMME, M.M.J. and SCHREURS, G.M.M.F. (1987): Structural investigations along a E–W cross-section in the Southern Ötztal Alps. In: FLÜGEL, H.W. and FAUPL, P. (eds): Geodynamics of the Eastern Alps, Deuticke-Wien, 214–225.

VERNON, R.H. (1976): Metamorphic processes. Wiley – New York, 247 pp.

VIELZEUF, D. (1984): Relations de phases dans le faciès granulite et implications géodynamiques. L'exemple des granulites des Pyrénées. B. Pascal Clermont-Ferrand.